PROSTHETICS

On prosthetic control: A regenerative agonist-antagonist myoneural interface

S. S. Srinivasan,[1,2] M. J. Carty,[2,3] P. W. Calvaresi,[2] T. R. Clites,[1,2] B. E. Maimon,[1,2] C. R. Taylor,[2,4] A. N. Zorzos,[2] H. Herr[2]*

Prosthetic limb control is fundamentally constrained by the current amputation procedure. Since the U.S. Civil War, the external prosthesis has benefited from a pronounced level of innovation, but amputation technique has not significantly changed. During a standard amputation, nerves are transected without the reintroduction of proper neural targets, causing painful neuromas and rendering efferent recordings infeasible. Furthermore, the physiological agonist-antagonist muscle relationships are severed, precluding the generation of musculotendinous proprioception, an afferent feedback modality critical for joint stability, trajectory planning, and fine motor control. We establish an agonist-antagonist myoneural interface (AMI), a unique surgical paradigm for amputation. Regenerated free muscle grafts innervated with transected nerves are linked in agonist-antagonist relationships, emulating the dynamic interactions found within an intact limb. Using biomechanical, electrophysiological, and histological evaluations, we demonstrate a viable architecture for bidirectional signaling with transected motor nerves. Upon neural activation, the agonist muscle contracts, generating electromyographic signal. This contraction in the agonist creates a stretch in the mechanically linked antagonist muscle, producing afferent feedback, which is transmitted through its motor nerve. Histological results demonstrate regeneration and the presence of the spindle fibers responsible for afferent signal generation. These results suggest that the AMI will not only produce robust signals for the efferent control of an external prosthesis but also provide an amputee's central nervous system with critical musculotendinous proprioception, offering the potential for an enhanced prosthetic controllability and sensation.

INTRODUCTION

Despite the increasing technological sophistication of limb prostheses, there has not been a commensurate decline in the rate of their rejection or abandonment by patients in the past 25 years (*1*). This problem is partially due to a mismatch between limitations imposed by the conventional amputation procedure and the high controllability demands of advanced limb prostheses. Contemporary prostheses often have multiple actuated degrees of freedom (DOFs), requiring consistent, isolated neural signals for their control (*1*–*3*). Current amputation surgical procedures are similar to those practiced 200 years ago and have not undergone significant evolution (*4*). Nerves are transected and buried within the residuum without end organs, often leading to the formation of painful neuromas (*2*, *5*, *6*). Muscles are severed at the amputation site and wrapped distally to create ample soft tissue padding for comfortable prosthetic socket use.

Electromyographic (EMG) signals from residual muscles are therefore limited in signal quality because the target muscles lie deep within the residuum and hence cannot be easily accessed, independently isolated, or measured consistently. Consequently, functional control of myoelectric prostheses through transdermal recording platforms, such as surface EMG (sEMG), is limited and users experience frustration due to poor prosthetic function (*7*). Furthermore, transdermal recording platforms cannot detect the relatively small signals within transected nerves without a muscle end organ. As a resolution to these difficulties, implanted and wireless approaches have been explored for the measurement of native EMG muscle signals, including implantable myoelectric sensors. These technologies are a critical step forward for the field but can only measure myoelectric signals from native musculature within the residuum (*8*). They cannot measure signals from transected motor nerves, which have no associated muscles with which to control the amputated part of the limb. Furthermore, this approach is often restricted to superficial muscles by power requirements and transmission limits of telemetry (*8*). To record directly from transected nerves, technologists have pursued implanted neural interfacing hardware, including fine wires, microchannels, arrays, and sieves. However, such techniques can be challenging due to biocompatibility problems, resolution and selectivity of fascicles, and signal magnitude. Implant-nerve interfacing often elicits neuroinflammatory foreign body responses, rendering nervous tissue pathologic and compromising the resulting signal (*9*, *10*). Even in the case of electrodes that are successful in chronic implantation, the number of fascicles in a given nerve (~100 s) presents a resolution and selectivity challenge (*11*). The signal magnitude from nerves is on the order of microvolts and can be easily corrupted by motion artifact, interference, and fibrotic responses. Therefore, although some studies have demonstrated successful chronic nerve cuff implantation, muscle-based electrodes are required for robust prosthetic control, due to the demand for stable, higher amplitude signals (*10*).

To mitigate the challenges associated with direct nerve recordings, a surgical technique called "targeted muscle reinnervation" (TMR) has been created, in which the neuromuscular tissue is reconfigured to shift efferent recording from nerves to muscles. Specifically, TMR involves surgically connecting transected nerves to surgically denervated muscles positioned superficially in an anatomical region proximal to the amputation site (*2*, *5*). sEMG measured from these superficial muscles is used to drive prosthetic motors. TMR has been shown to improve prosthetic limb control compared with traditional control techniques. However, the procedure requires denervating functional muscles, which may prove limiting as the number of actuated DOFs controlled by an external prosthesis increases (*5*).

[1]Harvard-MIT Division of Health Sciences and Technology, Massachusetts Institute of Technology, Cambridge, MA 02139, USA. [2]Center for Extreme Bionics, MIT Media Lab, Massachusetts Institute of Technology, Cambridge, MA 02139, USA. [3]Department of Plastic and Reconstructive Surgery, Brigham and Women's Hospital, Boston, MA 02115, USA. [4]Department of Media Arts and Sciences, Massachusetts Institute of Technology, Cambridge, MA 02139, USA.
*Corresponding author. Email: hherr@media.mit.edu

More recently, a regenerative peripheral nerve interface (RPNI) has been used for prosthetic limb control. To create an RPNI, a small, denervated, and devascularized muscle graft is innervated with a transected peripheral nerve. This muscle, once revascularized and reinnervated, provides a 1000-fold amplification of the nerve signal, precipitously increasing the signal-to-noise (SNR) ratio (*12*). RPNIs demonstrate marked neuroregenerative capacity and provide a robust method to amplify and record peripheral nerve signals for prosthetic control, without denervating functional native musculature (*12*, *13*). This technique has also been used to prevent neuroma formation of transected nerves in amputations. RPNIs allow specific nerves to be isolated and localized to a greater surface area (area of the muscle graft ~1 mm^2 versus area of nerve ~2 to 50 μm^2) for recording and stimulation (*12*, *13*). EMG electrodes implanted on these muscle grafts yield high signal fidelity in the chronic setting, exceeding 20 months (*14*). To date, more than 70 humans have benefitted from the implantation of RPNIs for neuroma ablation (*15*). Volitional control of a prosthesis driven by RPNI efferent signals has also been demonstrated in macaques and humans (*16*). RPNIs therefore have provided a more stable method of efferent signal interfacing.

However, the standard surgical paradigm, as well as TMR and RPNI approaches, lack the natural agonist-antagonist interaction inherent to intact biological limbs. The agonist-antagonist relationship enables the independent control of joint position and impedance. It also plays an essential role in musculotendinous proprioception, which is critical for the physiological sense of joint position, speed, and torque. In current amputation surgeries, the fundamental agonist-antagonist muscle pair architecture is severed. Therefore, when interfaced with a prosthesis, users have low-resolution motor control and rely heavily on visual feedback to guide their prosthetic limb, as opposed to the preferred natural sensory afferent feedback pathways enabled by agonist-antagonist muscle pairs (*17*–*19*). An amputation paradigm designed to reinstate this fundamental agonist-antagonist relationship would restore access to native afferent and efferent pathways for the advanced control of limb prostheses.

Proprioception is the body's natural method of relaying information about one's position and strength of effort to the central nervous system (CNS). Musculotendinous proprioception is crucial in optimizing autonomous, reflexive, and volitional motor control and trajectory planning (*20*, *21*). In their most basic mechanism, to create movement of a joint through its range of motion in the absence of a load, muscles act in agonist-antagonist pairs. When the agonist muscle, the prime mover, contracts, the antagonist muscle stretches. During this contraction, muscle spindle fibers and Golgi tendon organs transduce the stretch and force in the paired antagonist, respectively, which in turn transmit afferent signals to the CNS. These afferent signals, in addition to skin and joint receptors, convey limb position information, inform postural control, modulate joint stability, and enable an individual to effectively move and interface with the world (*22*). Although substituting or recreating sensory perception through external electrical or vibrotactile methods has been explored, restoring musculotendinous proprioception has not been effectively implemented. Natural musculotendinous proprioception is a critical component of feedback (*22*), and its restoration may improve prosthetic motor performance and provide a sense of ownership and embodiment between persons with amputation and their neurally interfaced prostheses.

Here, we describe the design of an agonist-antagonist myoneural interface (AMI), a surgical architecture designed to address the aforementioned challenges and enable bidirectional control of an external prosthesis. We validate the AMI's functionality in a murine model using electrophysiological, histological, and biomechanical methods.

Design of an AMI

The AMI reinstates agonist-antagonist muscle pairs to create a proxy joint controller within the residuum. In this architecture, two muscle grafts are surgically linked to form an agonist-antagonist pair placed subcutaneously, above the underlying fascia (Fig. 1). Each muscle pair serves as the target end organs for a transected flexor-extensor pair of motor nerves. Upon neural regeneration, the mature AMI is able to replicate physiological agonist-antagonist myoneural relationships within the residuum and convey bidirectional neural control information to and from an external limb prosthesis.

System-level implementation of AMI

In the envisioned implementation of the AMI in humans, volitional contraction of the agonist muscle causes a stretch in the antagonist (or vice versa), reproducing the physiological relationship that exists in the biological limb. EMG and fascicle state measurements (using implanted sensors) from both muscles are then used to provide efferent control of the prosthesis. Proprioceptive signals are naturally generated; passive extension of the antagonist muscle during agonist contraction causes mechanotransducers to generate physiologically relevant afferent signals of joint movement. To close the loop, afferent feedback from the prosthesis into the peripheral nervous system is achieved through functional electrical stimulation (FES) of the antagonist muscle (through implanted stimulation electrodes) to control the position or force applied on the mechanically linked agonist muscle (or vice versa). FES has been widely implemented in numerous therapeutic and prosthetic applications, including numerous U.S. Food and Drug Administration–approved devices for respiration, bladder control, ambulation, and restoring hand function (*23*–*26*). A full review of the stimulation methodology, advantages, and limitations can be found in (*23*).

This design enables robust efferent signal recording and natural proprioceptive afferent signal generation. We envision that interaction on this interface will facilitate the conversion of external prosthetic movement and environmental interaction into neural signals that readily integrate into an amputee's natural kinetic and kinematic frameworks.

Validation of the AMI

In this work, we performed the surgical creation of the AMI and characterized the healing and time course of reinnervation in a murine model. Additionally, we used electrophysiological techniques to evaluate the ability of the AMI to generate coupled agonist-antagonist motion, as well as graded efferent and afferent neural signals. Previously, the ability of an agonist-antagonist muscle pair to generate afferent signals correlated to stretch has been investigated in the absence of a joint (*27*). Surgically coapted muscles in a pulley-type fashion were stimulated to induce contraction and stretch in the agonist and antagonist muscles, respectively. This work comprises an expansion of the basic principles shown in (*27*), which were limited to natively innervated, vascularized muscle pairs. In this study, we hypothesized that the regenerated agonist muscle will produce a contraction correlated with the electrical activation of its motor nerve, resulting in a graded EMG signal and a correlated stretch of the antagonist muscle. We also anticipated that the AMI would provide afferent neural feedback that is monotonically increasing with increasing antagonist muscle stretch

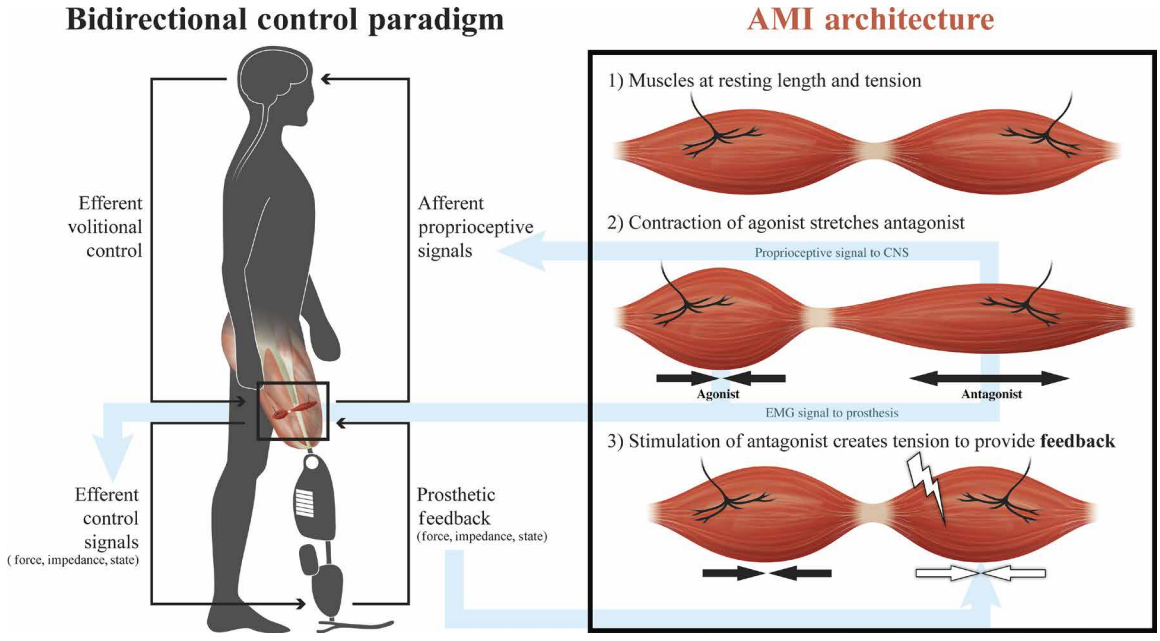

Fig. 1. AMI. AMI consists of two free muscle grafts linked in agonist-antagonist architecture and placed subdermally on underlying fascia. In the envisioned implementation, efferent control EMG signals from either muscle will be used to control the external prosthesis (position and impedance). Contraction of the agonist muscle will induce stretch and generate proprioceptive afferent signals in the antagonist muscle, which will provide the CNS with valuable information to improve motor control. Prosthetic feedback will be communicated to peripheral nervous system through FES of the antagonist muscle to control the position or force applied on the mechanically linked agonist muscle.

caused by the contraction of the linked agonist muscle. To test these hypotheses, we performed surgery in a murine model (n = 7), placing transected peroneal and tibial nerves into two separate denervated muscle masses linked by their tendons. After a 4- to 5-month postoperative regeneration period, we applied varying stimulation amplitudes to the regenerated motor nerve of the agonist muscle while measuring the agonist EMG signal. Simultaneously, we measured the electroneurographic (ENG) signal from the motor nerve innervating the antagonist, undergoing a mechanical stretch. Last, we performed histology of the harvested AMI to analyze healing and regeneration of the construct.

RESULTS

Surgical outcomes and reinnervation

After surgery, all rats recovered without incident, and none required secondary revision surgeries. Excluding the formation of a pressure sore in the calcaneal region due to denervation of the tibialis anterior and gastrocnemius muscles in three rats, the rats remained healthy for the experimental period of 4 months. The 14 muscle grafts created in this study demonstrated an average reduction of 52 ± 7% in size when compared with their size on creation (fig. S1). All grafts demonstrated signs of revascularization, as evidenced by gross inspection. Although a thin layer of fibrotic tissue encapsulated the agonist-antagonist muscles, they appeared nodular with well-demarcated margins. Gross morphology of tissues demonstrated resilient nervous tissue and firm linkage to the fascia. Insertional needle EMG was used to assess the health and reinnervation status of the muscles. While healthy innervated muscles are generally "electrically silent," denervated muscles demonstrate frequent, spontaneous depolarization (*28*). Monthly insertional needle EMG testing was performed, and the number of abnormal insertional events per unit time was measured, indicative of denervation (*28*). This frequency reached levels not significantly different from control muscles at 3 and 4 months, consistent with previously published results (fig. S2) (*12*).

Tendon-tendon coaptation facilitates independent innervation and insulates electrical cross-talk

In this surgical architecture, the tissue connecting the muscles was carefully selected for the important functions it performs. First, the tissue must isolate each muscle graft sufficiently to prevent any cross-innervation during the regeneration process (i.e., one nerve should not innervate both muscles). Additionally, for the muscles to provide accurate control EMG signals for an external prosthesis, the two grafts must be electrically insulated (i.e., when one muscle depolarizes, the other must not). We hypothesized that the tendinous tissue would sufficiently isolate each muscle.

We performed concurrent EMG recording from both the agonist and antagonist muscles while using a nerve stimulator (delivering 2-mA pulses) on one of the innervating nerves. Contraction was visually observed only in the agonist muscle innervated by the stimulated nerve. This confirmed that the peroneal and tibial nerves had selectively innervated the muscle grafts and no surrounding tissues. Furthermore, action potentials were generated in the agonist muscle, whereas the antagonist muscle remained electrically silent (Fig. 2), ensuring the availability of isolated EMG control signals for prosthetic control. We then stimulated nearby tissues, including the underlying fascia, biceps femoris (BF), and tibialis anterior, mimicking volitional contraction of muscles surrounding the AMI, and monitored for any coactivation of the AMI. No co-contraction or EMG signals were generated.

The surgical architecture demonstrates coupled motion and physiologically relevant strains

The surgical architecture explored in this work positioned the linked muscles in a linear arrangement, whereas the flexor-extensor muscles controlling joints in an intact limb are positioned in a shaft-pulley

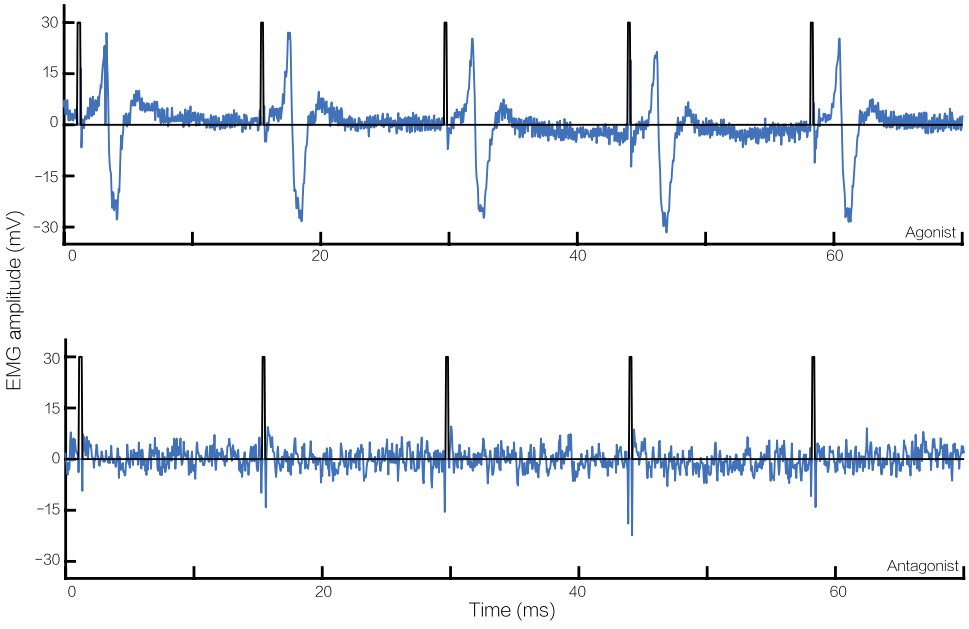

Fig. 2. Independently generated EMG. Action potentials (blue) are generated in the agonist muscle (top) upon 4-mA electrical stimulation pulses (black) but absent in the antagonist muscle (bottom) from a representative animal. Either muscle is electrically isolated by the insulation of the fascia and tendon-tendon coaptation, and therefore, contraction of the agonist does not cause co-contraction or electrical artifact in the antagonist muscle.

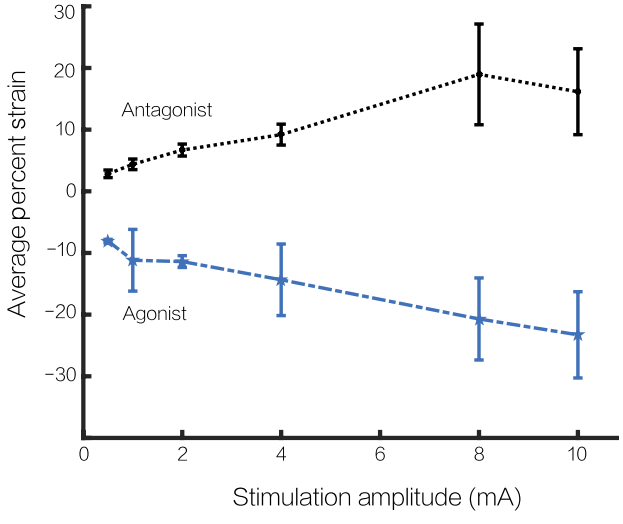

Fig. 3. Average strains generated by muscle grafts in the AMI. As contraction in the agonist increases in response to electrical stimulation ($n = 7$), stretch of the antagonist increases. Error bars represent SD.

structure. We localized the agonist-antagonist muscle pair on the fascia to facilitate natural sliding of the articulating surfaces. Stimulation of the agonist muscle yielded passive extension of the antagonist muscle, proportional in amplitude to agonist muscle excursion (movie S1). Fibrotic tissue did not significantly impede the contraction/excursion of the muscle pair. The range of the agonist-antagonist strains was measured between 0.08 ± 0.03 and 0.23 ± 0.14. For comparison, strains measured in human muscles induced by electrical stimulation are reported to be between 0.11 ± 0.02 and 0.3 ± 0.12 (*29*). As stimulation amplitude increased, average percent strain increased in the agonist muscle and created a proportional stretch in the antagonist muscle (Fig. 3). The ratio of antagonist to agonist muscle strain for each stimulation amplitude averaged 0.6 ± 0.2. The differences between strain levels at each stimulation level were found to be significant according to the analysis of variance (ANOVA) test ($P < 0.002$). Post hoc tests found significant differences at all stimulation levels except at 10 mA.

Generation of graded EMG signals

Stimulation was delivered using a hook electrode on each nerve, and EMG was measured from each muscle graft (Fig. 4). Evoked potentials averaged 5.7 ± 1.5 mV at the rheobase across all animals. Although the magnitude of EMG response varied from animal to animal, based on the graft size and location of EMG electrode, all animals showed linearly proportional increases in EMG amplitude with increased amplitudes of stimulation (average $r^2 = 0.85$ for $n = 7$) until the supramaximal stimulus, when EMG plateaued. A representative case of EMG measured from the agonist muscle is shown in Fig. 5. EMG morphology was normal, and no fatigue or reduction in amplitude was observed with repeated stimulation. SNR of evoked potentials averaged 65 dB. In all cases, no EMG spikes were observed in the antagonist muscle.

Graded afferent ENG signals suggest the generation of proprioceptive information

While the agonist muscle was being stimulated via a hook electrode on the innervating nerve, afferent signals from the nerve innervating the antagonist were recorded using a hook electrode (Fig. 4). Simultaneously, muscle excursion was measured. As stimulation intensity increased, the afferent signals generated from the antagonist muscle increased in amplitude (Fig. 6). Binned integration of rectified signals yielded gradation that correlated with the stretch of the antagonist. Linear regression yielded an $r^2 = 0.96$. As a control case and to identify any possible electrical artifact, the agonist-antagonist linkage was severed, by transecting the tendon-tendon coaptation, and the previous experiment was repeated. No extension was created in the antagonist muscle, and no afferent signals were generated (Fig. 6).

Immunostaining verifies neuronal reinnervation, spindle fiber regeneration, and regeneration

Intravital imaging of nerves traced with a biotinylated dextran amine (BDA) conjugated to Texas Red was performed on fresh tissue after euthanasia and demonstrated robust axonal regeneration within the muscle graft and localization on neuromuscular junctions (Fig. 7A). Hematoxylin and eosin (H&E) staining was also performed on the harvested AMI tissues. Nuclei lined up in a train-line fashion in the center of myocytes were found in several regions of muscle. This is indicative of young, regenerating or recovering myocytes, suggesting that, even at 5 months, there was ongoing regeneration of the muscle grafts (Fig. 7B) (*30*). Although several fully functional and intact blood vessels were found, there was also evidence of angioblasts and newly forming vascular

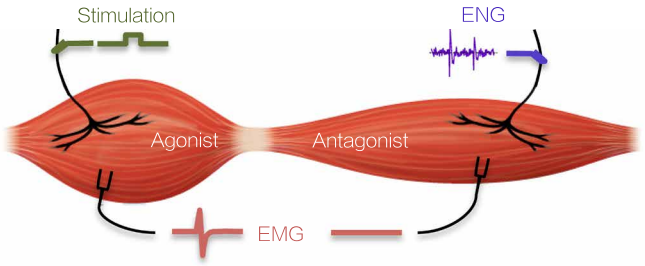

Fig. 4. Electrophysiological testing setup. A hook electrode is placed over both nerves to perform either stimulation or afferent ENG signal recording. Two EMG electrodes are placed in each muscle to record bipolar EMG. Under stimulation, we expect the agonist muscle to contract (left), generating EMG signal, and the antagonist muscle to stretch (right), generating ENG signal.

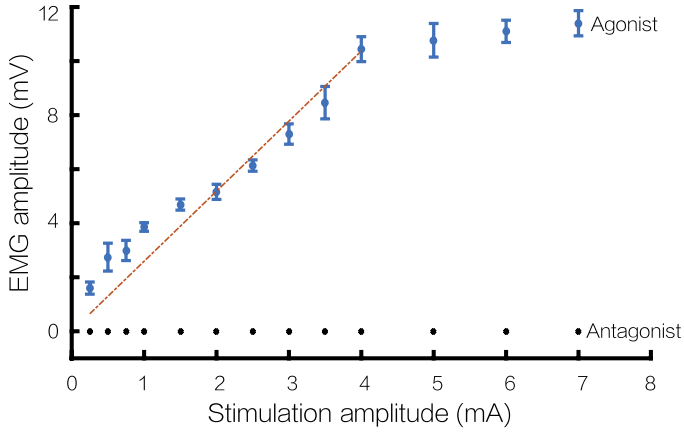

Fig. 5. Evoked potentials from agonist muscle grade with stimulation. Average peak EMG amplitude for each stimulation amplitude from a representative animal's agonist muscle demonstrates strong, positive, linear correlation ($r^2 = 0.85$) within the linear range. Stimulation amplitudes above 4 mA were supramaximal and were not regressed. No EMG spikes were generated in the antagonist muscle. Error bars represent SD.

beds (Fig. 7C). Spindle capsules and spindle fibers were also found in the H&E slides (Fig. 7D). Furthermore, at the point of coaptation, the tendons exhibited complete healing. The s46 dye was used to stain for spindle fibers and confirm the presence of this mechanotransducer, which is predominantly responsible for the generation of afferent signal (fig. S3). Staining yielded viable muscle spindle fibers localized among healthy myocytes in muscle cross sections (fig. S3).

DISCUSSION

The current surgical amputation paradigm is deficient in enabling effective bidirectional communication between the biological residuum and the worn prosthesis, and thereby limits the prosthetic motor control and feedback sensations afforded to the user (*18*, *31*). Bidirectional peripheral nerve communication will improve prosthesis functionality, enabling direct control of prosthetic actuators, and provide afferent sensation from the prosthesis. Here, we explore the design and behavior of an AMI, which generates not only isolated, graded EMG control signals from innervated muscle constructs but also afferent musculotendinous proprioceptive feedback.

In this investigation, a viable AMI was created using microneurosurgical techniques and evaluated through biomechanical, electrophysiological, and histological methods. In support of our hypothesis, upon nerve regeneration, the agonist muscle provided consistent contraction and graded efferent EMG signals corresponding to electrical stimulation of its regenerated motor nerve. We found that the gradation and resolution of efferent EMG signals were sufficiently granular ($P = 0.05$; SNR, 65 dB) to be meaningful for external prosthetic control (*32*). Additionally, our data support the hypothesis that afferent neural feedback measured from the antagonist nerve increases monotonically with increasing antagonist stretch, which is created by the contraction of the linked agonist muscle. Histological results confirmed the regenerative processes and the presence of spindle fibers.

Nerve regeneration and muscle atrophy

The time course of motor nerve regeneration and maturation of each muscle graft within the AMI was consistent with previously published results for regenerating muscle grafts in murine models (*11*, *14*). The regeneration period of neuromuscular constructs in humans is generally on the order of 6 to 12 months, a clinically acceptable and realistic time frame in the context of parallel rehabilitation measures for persons who have undergone limb amputation (*33*). Even with the level of atrophy observed in the murine model, the EMG signals generated by the muscles provided an SNR of 65 dB, which is more than sufficient for prosthetic control. Once reinnervation is complete (4 to 5 months), atrophy plateaus and the muscles begin to hypertrophy with use. In previous studies in macaques with reinnervating muscle tissue, even at 20 months, RPNIs were able to provide functional prosthesis commands (*14*). Additionally, on the basis of the viability of RPNIs in humans (*15*) and ability to provide efferent signals for prosthetic control (*16*), we do not expect the brief period of denervation atrophy in the AMI procedure to impede the AMI's functionality.

Anatomical placement of the AMI

In this study, the AMI was placed subdermally, which eased the measurement of insertional needle EMG throughout the course of the experiments. Additionally, the intentional attachment to underlying fascia, given its compliance and lubricious nature, yielded constructs that were able to sustain linear excursion. In future investigations, we anticipate that such a subdermal anatomical placement will facilitate isolated sEMG recordings, providing the potential for a completely transdermal interfacing approach.

Translation to humans

This study demonstrates that the AMI is a technically tractable procedure with broad applicability and minimal risk, lending itself to rapid translation to human implementation. The following factors specifically ease translation:

(i) Tissue requirements for construction of the AMI are minimal, requiring only native nerve and the recruitment of small segments of muscle. The muscle grafts required for the AMI procedure can be procured from anywhere in the body. In contrast to TMR (*2*, *5*), which is beholden to native body architecture and the availability of muscle near the site of amputation, the AMI can be constructed anywhere in the residual limb.

(ii) The footprint of each AMI is small [each muscle graft ~4 cm × 1.5 cm in humans (*15*)], enabling the construction of multiple AMIs for the control of multiple prosthetic DOFs. Given the relatively limited anatomic space available in residual limbs, the small footprint of the AMI is of paramount importance for achieving robust functionality.

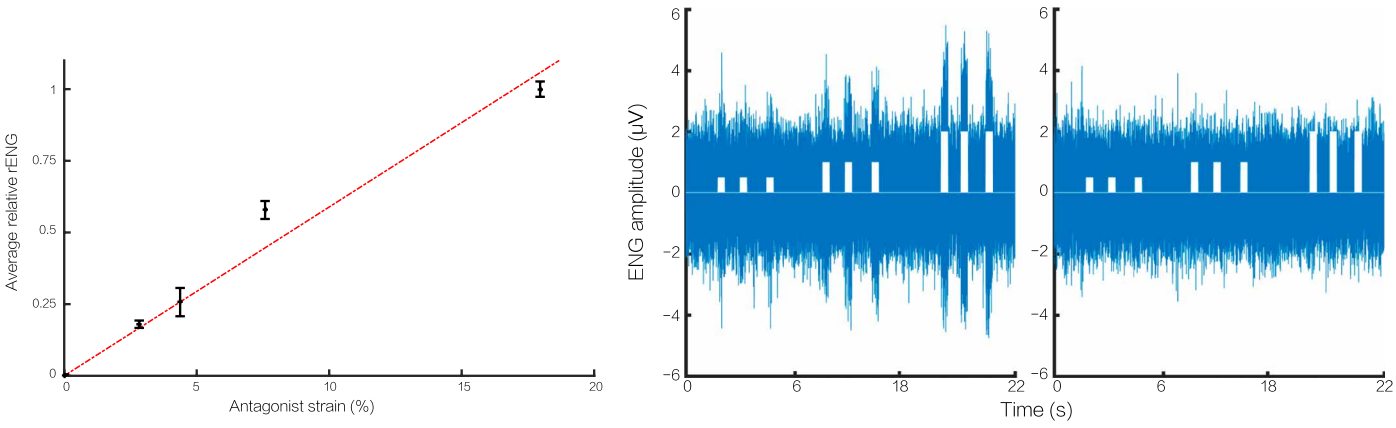

Fig. 6. Afferent signals generated from antagonist correlate with muscle strain. (**Left**) The average rectified ENG (rENG) amplitudes in response to increasing antagonist stretch amplitudes from $n = 7$ animals are shown and correlate linearly ($r^2 = 0.96$). (**Center**) Raw afferent activity originating from stretch response in the antagonist muscle demonstrates gradation. (**Right**) As a control case, in which the agonist-antagonist is severed, no afferent signals result, even when agonist muscle is stimulated. Stimulation pulses were delivered at 0.5, 1, and 2 mA (white). Error bars represent SD.

(iii) AMIs can be incorporated into acute amputations and revision procedures in patients' residual limbs, given its modest tissue requirements. Furthermore, in revision procedures, the AMI can be implemented at any level of amputation, using the neural structures that remain viable. This is true in the case of both upper and lower extremity amputations and makes the AMI applicable to a wide range of patient cases.

(iv) The AMI surgery is inherently low risk. Because this procedure merely rearranges distal tissues in a functional architecture, the failure of the AMI to function properly will result in degeneration into benign scar tissue, with relatively little negative sequelae for the patient and possible neuroma prophylaxis. This makes the AMI a low-risk option for nearly all amputees except those with known neuropathic diseases.

Overall, the AMI's minimal requirements and adaptability make it a highly scalable approach for a broad range of patient cases. Furthermore, previous studies in RPNIs have progressed directly from murine models to humans (*15*, *16*), suggesting that this technique readily lends itself to translation.

AMI integration with CNS

In the realm of neuroplasticity after an amputation, the AMI presents a number of clear benefits over existing approaches and promotes functional recovery. We anticipate that the use of native flexor and extensor nerves, and the ability of regenerative muscle to take on the firing characteristics of the innervating nerve, will preclude the need for an amputee's CNS to undergo any "rewiring." Additionally, given the use of native nerves, the transition from pre-amputation to post-amputation control of an external prosthesis is expected to be seemingly natural, a significant advantage when compared with many current methods (*34*). Moreover, in contrast to current methods of providing vibrotactile or electrotactile stimulation to restore proprioception, the generation of natural proprioceptive signals may be intuitive and require less neuroplastic modification (*31*, *34*–*36*). Last, because FES will occur on the muscle grafts, and not directly on nerves, the AMI circumvents the potential elicitation of pain through afferent nociceptive pathways caused by electrical stimulation. Especially with implanted intramuscular electrodes, FES has been shown to be efficacious in inducing repeatable contractions with little pain production because it bypasses sensory afferent channels (*23*).

How might a prosthesis be controlled using an AMI?

The AMI is unique in its potential to use native tissue mechanoreceptors to translate prosthetic sensory information related to muscle stretch and tension into neural signals similar to those experienced in the normal biological milieu. In contrast to alternative afferent feedback approaches that bypass native biological end organs (*31*), the AMI incorporates the specialized biomechanical structures inherently present in muscle to transduce information regarding muscle fascicle state and force. The AMI opens the door for a variety of biomimetic neural control architectures for advanced prosthetic systems. Here, we describe several prosthetic control implementations as an exploration of how the AMI might be operationalized.

Appropriate sensorization is essential for the adequate transmission of neural signals to and from AMI constructs within the residual limb. One of the distinct benefits of the AMI over direct nerve interfacing is the isolation of implanted synthetic sensors to muscle tissue, thereby sparing the more fragile neural tissue of potential biocompatibility and mechanical loading effects. Additionally, interfacing with muscles enables the system to take advantage of muscle mechanotranducers' capability to transduce muscle force, position, velocity, and other components into a comprehensive signal to the various fascicles of its innervating nerve. In contrast, directly interfacing with fascicles in nerves would require recapitulation of this complex mechanotransduction and transmission to the appropriate fascicles with high specificity. We envision a system in which, within each AMI, an array of sensors and stimulators is placed to achieve robust control fidelity between the AMI and the external prosthetic device. Electrodes placed on each muscle of the agonist-antagonist pair record EMG, which is used for motor intent recognition as a prosthetic control signal. In addition, these same muscle electrodes will apply FES for sensory feedback from an external prosthesis. Electrodes placed on the muscle will scar into place, minimizing motion artifact. Both invasive and noninvasive electrodes can be used; in the noninvasive approach, sEMG electrodes positioned on the skin surface adjacent to the muscle grafts would isolate sEMG and apply FES. To achieve closed-loop control of FES, fascicle state and force sensing of each muscle within the AMI are also necessary. Fascicle state sensing could be achieved using sonomicrometry crystals stitched into muscle fibers (*27*); muscle force would then be estimated using a

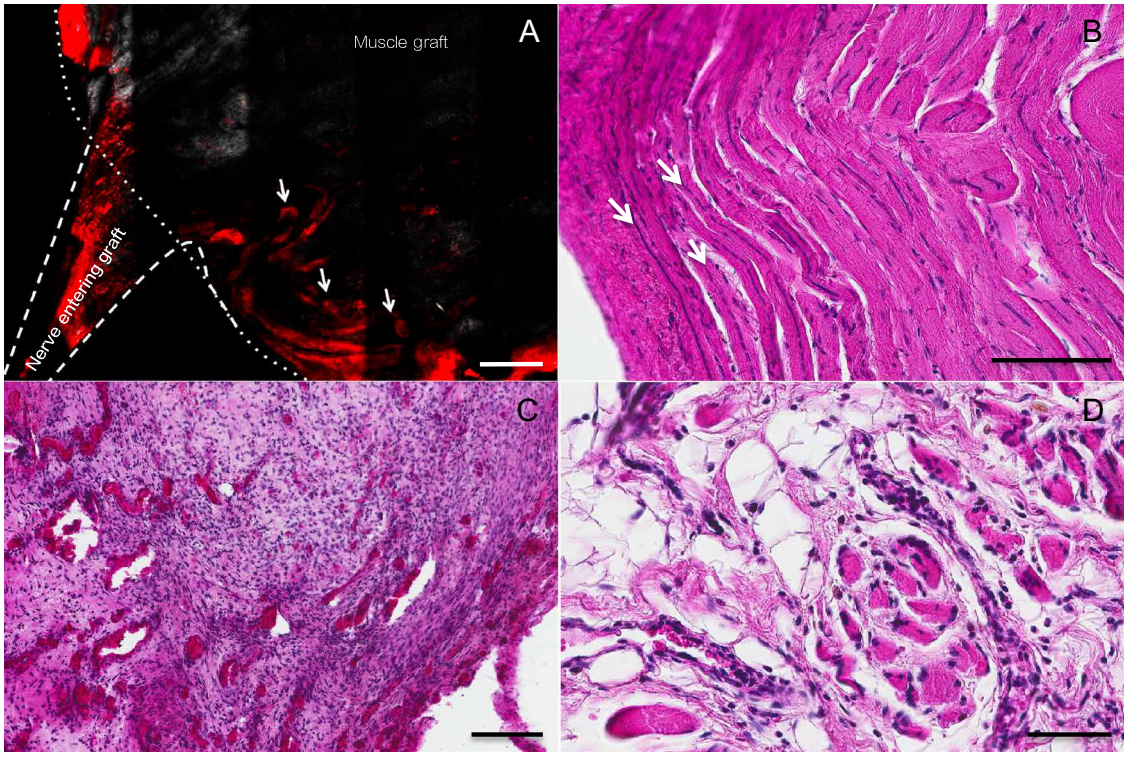

Fig. 7. Histology demonstrates reinnervation, regeneration, and revascularization. (**A**) Nerve staining in a cross section of the AMI shows innervating tracts and multiple synapses onto neuromuscular junctions in the muscle graft, as indicated by arrows. Scale bar, 1 mm. (**B**) H&E stain shows myocytes with centrally located nuclei in a train-line fashion (indicated by arrows), suggesting ongoing regeneration of myocytes. Scale bar, 100 μm. (**C**) Angioblasts found near the periphery demonstrate regenerating vascular vessels. Scale bar, 200 μm. (**D**) Regenerated spindle fibers and spindle capsule in a cross section of the muscle graft. Scale bar, 50 μm.

biophysical muscle model (e.g., Hill muscle model) with measured EMG and fascicle state as model inputs.

With adequate sensor placement and stability, we envision direct proportional control paradigms for the external prosthesis. For example, using EMG and sonomicrometry sensors, a master-slave control paradigm could be used between an AMI and a prosthetic joint. In this paradigm, agonist-antagonist lengths and speeds, measured using sonomicrometry, could be used as control targets by the external bionic limb processors; motors on the prosthesis would be driven to output bionic limb joint positions and speeds corresponding to targets obtained using an anatomically derived transformation from the linear muscle space of the AMI to the prosthetic rotary joint space. In another controller implementation, agonist-antagonist AMI force could be estimated from EMG and sonomicrometry, scaled via a biophysical model to represent forces from analogous muscles within an intact physiological limb, and used to directly control prosthetic joint torque and impedance.

The AMI also plays an important role in providing afferent neural feedback from the external prosthesis. FES provides a modality for this interface. In practice, force information from synthetic sensors on the corresponding prosthetic joint would be used to drive stimulation of the antagonist muscle of an AMI, allowing control of the force within the coupled agonist by the external prosthetic processors. For example, when an upper extremity prosthetic user picks up a barbell weight and flexes her prosthetic wrist, the AMI corresponding to wrist flexors-extensors is electrically stimulated to allow the user to experience the barbell weight; as the AMI agonist muscle contracts, an FES control is applied to the AMI antagonist muscle, increasing the force borne by the agonist muscle. This FES signal is modulated proportional to the error between the measured bionic wrist force and the measured force from AMI muscle fiber sensors.

An alternative approach to FES control of afferent sensation involves direct modulation of stretch in the agonist-antagonist muscles of the AMI, by creating a closed-loop control system using the measured fascicle states from sonomicrometry (*27*). Consider the experience of shaking hands with another person: If a person grasps the bionic hand of the prosthetic user, such a handshake may forcibly change the positions of the bionic joints, as would happen in a handshake between two persons with intact biological limbs. These changes in joint position must be reflected in the agonist-antagonist muscles in order for the prosthetic user to receive accurate proprioceptive feedback. In the proposed paradigm, joint state information from position sensors within the bionic limb would generate position and speed targets for an FES control applied to the AMI muscles. For example, if the handshake flexes the bionic wrist, the FES controller would receive bionic wrist state information from a synthetic sensor within the wrist and apply an electrical activation to the agonist AMI muscle proportional to the error between the measured bionic wrist state and the measured state from muscle fiber state sensors. This activation would cause the agonist muscle to contract, thereby stretching the antagonist. The prosthetic user would experience this change in relative AMI muscle state as a change in the position of their bionic wrist, through afferent feedback from muscle spindle receptors in the agonist-antagonist pair.

All of these proposed control and feedback methodologies are scalable across multiple DOFs at all levels of amputation. In a multi-DOF system, one AMI is created in the residual limb for each DOF to be controlled. In summary, integration of the AMI architecture into a prosthetic control system is an obvious extension of the work presented in this manuscript. This study validates the critical biomechanical and electrophysiological capabilities necessary for the aforementioned control architecture.

Summary and future work

In this study, validation of the AMI resulted in graded efferent EMG and afferent ENG signals generated from functionally regenerated myoneural constructs. Once translated to the clinic, the AMI framework has the potential to enable more robust, reliable, and intuitive communication between a person with limb amputation and their external prosthesis. Physiologically meaningful musculotendinous proprioception will likely have a marked impact on reflex control, fine volitional motor control, trajectory planning, and overall user experience (*21*, *37*). Further work on muscle spindle regeneration characteristics and the contribution of the Golgi tendon organs within the AMI would yield valuable insights into the afferent signaling mechanisms in regenerating muscle grafts. The direct benefits of proprioception generated through agonist-antagonist muscle could be explored through large animal or human studies comparing linked and unlinked muscle grafts. Additionally, implementation in humans will shed light on the actual perception generated by the AMI. In summary, the AMI's capacity for bidirectional communication enables high-fidelity prosthetic control from transected motor nerves.

MATERIALS AND METHODS

Study design

Our central hypothesis is that muscle grafts linked in an agonist-antagonist pair can generate physiologically relevant strain rates, graded efferent EMG signals from the agonist, and graded afferent ENG resulting from the antagonist muscle in response to electrical stimulation. We performed surgery in a murine model and evaluated outcomes at a 4- to 5-month time point. All animal experiments were conducted under the supervision of the Committee on Animal Care at the Massachusetts Institute of Technology (MIT) on a 5-month-old male Lewis rats, weighing between 325 and 364 g.

Surgical procedure: Creation of agonist-antagonist muscle grafts

Rats ($n = 7$) were anesthetized with 1 to 2% isoflurane. A curvilinear incision was performed on the right distal hindlimb to expose the anterior and posterior muscle groups. The extensor digitorum longus muscle was isolated and disinserted, with care taken to preserve tendinous tissue. The weight and length of the muscle were measured and recorded. Myotomy of the extensor digitorum longus muscle created two equally sized muscle grafts. Tendons from each segment were coapted to form the linked agonist-antagonist muscle pair. Intermuscular dissection revealed the tibial and common peroneal nerves, which were carefully separated from the connective tissue and transected as distally as possible. These nerves were brought up through the BF. The muscle grafts were freely transferred and sutured (5-0 Nylon) to the ipsilateral fascia overlaying the BF, mirroring its original orientation. A superficial myotomy was performed through the epimysium of each muscle segment to neurotize with either the peroneal or tibial nerve (8-0 microsuture) and create two distinct muscle grafts (fig. S4). The incision was closed using a 4-0 suture.

Assessing reinnervation through insertional needle EMG

Starting 1 month postoperatively, insertional needle EMG was performed to monitor the muscle grafts for signs of denervation (*12*). Rats were anesthetized under 1 to 2% isoflurane, and the AMI was identified by either palpation or a small incision in the hindlimb, which exposed the grafts. A 30-gauge needle was positioned on a stabilization apparatus. This was inserted into one of the muscle grafts, and EMG was recorded for a 2-min window. A brief version of this procedure is demonstrated in movie S2. This procedure was performed three times on each graft and contralateral muscle each month. The frequency of insertional activity was quantified as a number of events (fibrillation potentials, positive sharp waves, fasciculations, etc.) per time, and trends were analyzed over time.

Assessing excursion, coupled motion, and strain

Excursion and strain rates of the architecture were quantified to assess the AMI's ability to provide graded signals for the control of a prosthesis. In a terminal experiment, the AMI was exposed by retracting the skin from the ankle to knee joint. An incision at the medial aspect of the BF allowed access to the peroneal and tibial nerves under the BF. Connective tissue was excised, both nerves were isolated, and a nerve hook electrode was placed on the nerve and insulated with mineral oil (Sigma). Endpoints of the AMI and tendon-tendon coaptation point were labeled with a surgical marker. The muscle grafts of the AMI were stimulated using a nerve hook electrode at increasing stimulation amplitudes. Concomitant video recording was performed with a Nikon D3200 digital single-lens reflex camera positioned orthogonally to the animal's hindlimb to ensure accurate linear strain measurements. Monophasic muscle stimulation was delivered by a commercial muscle stimulator (NL800, Digitimer), with stimulation parameters controlled digitally using a custom program on the myRIO processor (National Instruments). Using image processing on ImageJ, the length between marked points in this linear architecture was calculated during rest and stimulation to yield absolute and relative values of excursion and strain.

Electrophysiology: Efferent and afferent signal measurement

Two 30-gauge EMG needles (Natus Medical) were carefully inserted near the middle of each muscle graft for bipolar recording. A ground electrode was placed subcutaneously in the back. EMG and stimulation signals were recorded on a 20 kS/s multichannel amplifier with a fixed 200× gain (Intan Technologies) and analyzed in MATLAB. To identify whether the muscle grafts were electrically isolated, a stimulation pulse was applied and EMG from both muscles was recorded; clear evoked EMG in the stimulated muscle and electrical silence in the antagonist muscle would evidence electrical isolation. Further, stimulation at increasing amplitudes was delivered (0.5 to 10 mA; 100- and 200-μs pulses) and resulting EMG was measured. Electrophysiological testing parameters were chosen in accordance with previous studies in RPNIs as well as the range acceptable for muscle/nerve tissue (*12*, *38*). In a separate set of tests, afferent signals generated by the antagonist muscles were recorded using a hook electrode on the antagonist nerve (Fig. 4).

Next, as a negative control, to test the linking strategy's role in creating coupled motion and agonist stretch, the tendon-tendon coaptation was transected. Stimulation pulses were again delivered, and the resulting afferent signals and EMG were measured.

Afferent electroneurographic differential signals were preamplified (Grass P511 AC Amplifier, Grass Instruments), passed through a sample-and-hold blanking circuit, bandpass-filtered (0.3 to 3 kHz), and amplified (RHD2000, Intan Technologies) before being recorded. The blanking circuit silenced the preamplifier for 200 to 400 μs after each stimulation pulse to prevent amplifier saturation and corruption of ENG signal by electrical noise from the stimulation. Digital data processing included a software blank of 400 μs to ensure that any stimulation artifact was removed. ENG signals were bandpass-filtered (0.3 to 3 Hz), digitally rectified, and bin integrated using a window of 250 μs. Data from

all animals were normalized to a range of 0 to 1 by setting the peak signal at the maximal stimulation amplitude to 1.

Atrophy

Photographs and measurements of the AMI were taken during surgery and at the terminal harvest to quantify the change in size of the AMI, based on length and width.

Histology

For two animals, nerve tracing was performed using BDA conjugated to Texas Red (Thermo Fisher). A 2.5% (w/v) solution of BDA–Texas Red was created in double-distilled water. Two days before terminal harvest, 10 µl was injected into the proximal tibial and peroneal nerves innervating the muscle grafts at a rate of 1 µl/min using a 10-µm tip. The needle was held in place for 3 min before removal to minimize leakage of the dye back through the insertion tract. Intravital imaging was performed on an Olympus FV1000MPE microscope (Olympus Americas, Waltham, MA) using a 25×, numerical aperture 1.05 water objective. Excitation was achieved using a DeepSee Tai-sapphire femtosecond pulse laser (Spectra-Physics, Santa Clara, CA) at 840 nm. The emitted fluorescence was collected using photomultiplier tubes with emission filters of 425/30 nm for collagen 1, 525/45 nm for tissue autofluorescence, and 607/70 nm for BDA–Texas Red. Collagen 1 was excited by second harmonic generation and emits as polarized light at half the excitation wavelength. Stitched images were created in the Olympus FV10 software by collecting multiple consecutive fields and using the stitching algorithm in the program. All images were processed using ImageJ.

For all animals, at the end of all terminal testing, the AMI and innervating nerves were harvested and fixed in 4% paraformaldehyde for 24 hours, paraffin processed, embedded, and sectioned at 5 µm. Five selected sections from each animal were stained with H&E to identify general morphology of muscle and nerve tissues as well as identify the presence of neovasculature, muscle spindles, and myocyte health. Five sections were also stained with s46 (Developmental Studies Hybridoma Bank) using a 1:200 dilution of the supernatant in blocking buffer to identify muscle spindle fibers. A goat anti-mouse green fluorescent protein secondary antibody was used.

Statistical analysis

Unless otherwise noted, we used a Student's *t* test at an α of 0.05 to test for significance.

SUPPLEMENTARY MATERIALS

robotics.sciencemag.org/cgi/content/full/2/6/eaan2971/DC1
Fig. S1. AMI structure at surgery and harvest.
Fig. S2. Time course of denervation.
Fig. S3. Staining (s46) for spindle fibers.
Fig. S4. AMI structure (left) and surgery in murine model (right).
Movie S1. Antagonist-agonist muscles demonstrate coupled motion.
Movie S2. Insertional needle EMG recording procedure.

REFERENCES AND NOTES

1. E. A. Biddiss, T. T. Chau, Upper limb prosthesis use and abandonment: A survey of the last 25 years. *Prosthet. Orthot. Int.* **31**, 236–257 (2007).
2. T. A. Kuiken, G. Li, B. A. Lock, R. D. Lipschutz, L. A. Miller, K. A. Stubblefield, K. B. Englehart, Targeted muscle reinnervation for real-time myoelectric control of multifunction artificial arms. *JAMA* **301**, 619–628 (2009).
3. A. E. Schultz, T. A. Kuiken, Neural interfaces for control of upper limb prostheses: The state of the art and future possibilities. *PM&R* **3**, 55–67 (2011).
4. B. J. Brown, M. L. Ioro, M. Klement, M. R. C. Mica, A. El-Amraoui, P. O'Halloran, C. E. Attinger, Outcomes after 294 transtibial amputations with the posterior myocutaneous flap. *Int. J. Low. Extrem. Wounds* **13**, 33–40 (2014).
5. J. E. Cheesborough, L. H. Smith, T. A. Kuiken, G. A. Dumanian, Targeted muscle reinnervation and advanced prosthetic arms. *Semin. Plast. Surg.* **29**, 62–72 (2015).
6. J. H. Ko, P. S. Kim, K. D. O'Shaughnessy, X. Ding, T. A. Kuiken, G. A. Dumanian, A quantitative evaluation of gross versus histologic neuroma formation in a rabbit forelimb amputation model: Potential implications for the operative treatment and study of neuromas. *J. Barchial Plex. Peripher. Nerve Inj.* **6**, 8 (2011).
7. C. Pylatiuk, S. Schulz, L. Döderlein, Results of an internet survey of myoelectric prosthetic hand users. *Prosthet. Orthot. Int.* **31**, 362–370 (2007).
8. R. F. Weir, P. R. Troyk, G. A. DeMichele, D. A. Kerns, J. F. Schorsch, H. Maas, Implantable myoelectric sensors (IMESs) for intramuscular electromyogram recording. *IEEE Trans. Biomed. Eng.* **56**, 159–171 (2009).
9. W. M. Grill, S. E. Norman, R. V. Bellamkonda, Implanted neural interfaces: Biochallenges and engineered solutions. *Annu. Rev. Biomed. Eng.* **11**, 1–24 (2009).
10. M. Ortiz-Catalan, R. Brånemark, B. Håkansson, J. Delbeke, On the viability of implantable electrodes for the natural control of artificial limbs: Review and discussion. *Biomed. Eng. Online* **11**, 33 (2012).
11. D. K. Leventhal, D. M. Durand, in *Proceedings of the Second Joint 24th Annual Conference and the Annual Fall Meeting of the Biomedical Engineering Society Engineering in Medicine and Biology* (2002), vol. 3, pp. 2058–2059.
12. T. A. Kung, N. B. Langhals, D. C. Martin, P. J. Johnson, P. S. Cederna, M. G. Urbanchek, Regenerative peripheral nerve interface viability and signal transduction with an implanted electrode. *Plast. Reconstr. Surg.* **133**, 1380–1394 (2014).
13. M. G. Urbanchek, T. A. Kung, C. M. Frost, D. C. Martin, L. M. Larkin, A. Wollstein, P. S. Cederna, Development of a regenerative peripheral nerve interface for control of a neuroprosthetic limb. *Biomed. Res. Int.* **2016**, 5726730 (2016).
14. N. B. Langhals, S. L. Woo, J. D. Moon, J. V. Larson, M. K. Leach, P. S. Cederna, M. G. Urbanchek, Electrically stimulated signals from a long-term regenerative peripheral nerve interface, *2014 36th Annual International Conference of the IEEE* (IEEE, 2014), pp. 1989–1992.
15. Z. T. Irwin, K. E. Schroeder, P. P. Vu, D. M. Tat, A. J. Bullard, S. L. Woo, I. C. Sando, M. G. Urbanchek, P. S. Cederna, C. A. Chestek, Chronic recording of hand prosthesis control signals via a regenerative peripheral nerve interface in a rhesus macaque. *J. Neural Eng.* **13**, 046007 (2016).
16. M. G. Urbanchek, I. C. Sando, Z. T. Irwin, P. Vu, S. L. Woo, C. A. Chestek, P. S. Cederna, Validation of regenerative peripheral nerve interfaces for control of a myoelectric hand by macaques and human. *Plast. Reconstr. Surg. Glob. Open.* **4**, 69 (2016).
17. C.-H. Blanc, O. Bürens, Amputations of the lower limb—An overview on technical aspects. *Acta Chir. Belg.* **104**, 388–392 (2004).
18. F. Cordella, A. L. Ciancio, R. Sacchetti, A. Davalli, A. G. Cutti, E. Guglielmelli, L. Zollo, Literature review on needs of upper limb prosthesis users. *Front. Neurosci.* **10**, 209 (2016).
19. A. L. Ciancio, F. Cordella, R. Barone, R. A. Romeo, A. D. Bellingegni, R. Sacchetti, A. Davalli, G. Di Pino, F. Ranieri, V. Di Lazzaro, E. Guglielmelli, L. Zollo, Control of prosthetic hands via the peripheral nervous system. *Front. Neurosci.* **10**, 116 (2016).
20. S. Raspopovic, M. Capogrosso, F. M. Petrini, M. Bonizzato, J. Rigosa, G. Di Pino, J. Carpaneto, M. Controzzi, T. Boretius, E. Fernandez, G. Granata, C. M. Oddo, L. Citi, A. L. Ciancio, C. Cipriani, M. C. Carrozza, W. Jensen, E. Guglielmelli, T. Stieglitz, P. M. Rossini, S. Micera, Restoring natural sensory feedback in real-time bidirectional hand prostheses. *Sci. Transl. Med.* **6**, 222ra19 (2014).
21. B. L. Riemann, S. M. Lephart, The sensorimotor system, part II: The role of proprioception in motor control and functional joint stability. *J. Athl. Train.* **37**, 80–84 (2002).
22. U. Proske, S. C. Gandevia, The proprioceptive senses: Their roles in signaling body shape, body position and movement, and muscle force. *Physiol. Rev.* **92**, 1651–1697 (2012).
23. P. H. Peckham, J. S. Knutson, Functional electrical stimulation for neuromuscular applications. *Annu. Rev. Biomed. Eng.* **7**, 327–360 (2005).
24. M. Fall, S. Lindström, Functional electrical stimulation: Physiological basis and clinical principles. *Int. Urogynecology J.* **5**, 296–304 (1994).
25. L. Meng, B. Porr, C. A. Macleod, H. Gollee, A functional electrical stimulation system for human walking inspired by reflexive control principles. *Proc. Inst. Mech. Eng.* [H]. **231**, 315–325 (2017).
26. H. Kern, C. Hofer, M. Mödlin, C. Forstner, D. Raschka-Högler, W. Mayr, H. Stöhr, Denervated muscles in humans: Limitations and problems of currently used functional electrical dtimulation training protocols. *Artif. Organs* **26**, 216–218 (2002).
27. T. R. Clites, M. J. Carty, S. Srinivasan, A. N. Zorzos, H. M. Herr, A murine model of a novel surgical architecture for proprioceptive muscle feedback and its potential application to control of advanced limb prostheses. *J. Neural Eng.* **14**, 036002 (2017).
28. D. I. Rubin, Needle electromyography: Basic concepts and patterns of abnormalities. *Neurol. Clin.* **30**, 429–456 (2012).

29. X. Deligianni, M. Pansini, M. Garcia, A. Hirschmann, A. Schmidt-Trucksäss, O. Bieri, F. Santini, Synchronous MRI of muscle motion induced by electrical stimulation. *Magn. Reson. Med.* **77**, 664–672 (2017).
30. S. B. P. Chargé, M. A. Rudnicki, Cellular and molecular regulation of muscle regeneration. *Physiol. Rev.* **84**, 209–238 (2004).
31. T. A. Kuiken, P. D. Marasco, B. A. Lock, R. N. Harden, J. P. A. Dewald, Redirection of cutaneous sensation from the hand to the chest skin of human amputees with targeted reinnervation. *Proc. Natl. Acad. Sci. U.S.A.* **104**, 20061–20066 (2007).
32. C. J. De Luca, Surface electromyography: Detection and recording (DelSys, 2002); www.delsys.com/Attachments_pdf/WP_SEMGintro.pdf.
33. American Academy of Orthotists and Prosthetists, Stages of care—Postoperative management of the lower extremity amputation (2014); www.oandp.org/olc/lessons/html/SSC_02/07stages.asp?frmCourseSectionId=514F4373-8EDF-434A-BA08-C221FA8ABD71.
34. G. Di Pino, E. Guglielmelli, P. M. Rossini, Neuroplasticity in amputees: Main implications on bidirectional interfacing of cybernetic hand prostheses. *Prog. Neurobiol.* **88**, 114–126 (2009).
35. G. S. Dhillon, K. W. Horch, Direct neural sensory feedback and control of a prosthetic arm. *IEEE Trans Neural. Syst. Rehabil. Eng.* **13**, 468–472 (2005).
36. P. D. Marasco, K. Kim, J. E. Colgate, M. A. Peshkin, T. A. Kuiken, Robotic touch shifts perception of embodiment to a prosthesis in targeted reinnervation amputees. *Brain* **134**, 747–758 (2011).
37. M. A. Pet, J. H. Ko, J. L. Friedly, P. D. Mourad, D. G. Smith, Does targeted nerve implantation reduce neuroma pain in amputees? *Clin. Orthop.* **472**, 2991–3001 (2014).
38. J. T. Mortimer, D. Kaufman, U. Roessmann, Intramuscular electrical stimulation: Tissue damage. *Ann. Biomed. Eng.* **8**, 235–244 (1980).

Acknowledgments: We thank A. Amato and P. Cederna for their consultation on neurophysiological signals and regenerative peripheral neural interfaces. We thank the Koch Institute Swanson Biotechnology Center for technical support on histology and intravital imaging services. **Funding:** This work was funded by the MIT Media Lab Consortia.
Author contributions: S.S.S. performed the experimental conception and design, surgeries, data collection, analysis, documentation, and writing of the paper. M.J.C. contributed to conceptualization of the AMI and surgeries. P.W.C. assisted with data collection. A.N.Z. and T.R.C. assisted with experimental design and writing of the paper. H.H. conceived the AMI architecture as well as contributed to the experimental design and writing of the paper. B.E.M. assisted with histology. C.R.T. designed the electrical stimulator used in experimentation.
Competing interests: The authors declare that they have no competing interests.
Data and materials availability: All data for the conclusion in the paper are present in the paper and/or Supplementary Materials. Contact S.S.S. for additional information.

Submitted 24 March 2017
Accepted 10 May 2017
Published 31 May 2017
10.1126/scirobotics.aan2971

Citation: S. S. Srinivasan, M. J. Carty, P. W. Calvaresi, T. R. Clites, B. E. Maimon, C. R. Taylor, A. N. Zorzos, H. Herr, On prosthetic control: A regenerative agonist-antagonist myoneural interface. *Sci. Robot.* **2**, eaan2971 (2017).

Science Robotics

On prosthetic control: A regenerative agonist-antagonist myoneural interface

S. S. Srinivasan, M. J. Carty, P. W. Calvaresi, T. R. Clites, B. E. Maimon, C. R. Taylor, A. N. Zorzos, and H. Herr

Sci. Robot. **2** (6), eaan2971. DOI: 10.1126/scirobotics.aan2971

Science Robotics (ISSN 2470-9476) is published by the American Association for the Advancement of Science. 1200 New York Avenue NW, Washington, DC 20005. The title *Science Robotics* is a registered trademark of AAAS.